ELSEVIER

FEMS Microbiology Ecology 52 (2005) 185–195

FEMS MICROBIOLOGY Ecology

www.fems-microbiology.org

Diversity and vertical distribution of magnetotactic bacteria along chemical gradients in freshwater microcosms

Christine B. Flies, Henk M. Jonkers, Dirk de Beer, Katja Bosselmann, Michael E. Böttcher, Dirk Schüler *

Max Planck Institute for Marine Microbiology, Celsiusstr. 1, D-28359, Bremen, Germany

Received 24 August 2004; received in revised form 1 November 2004; accepted 3 November 2004

First published online 26 November 2004

Abstract

The vertical distribution of magnetotactic bacteria along various physico-chemical gradients in freshwater microcosms was analyzed by a combined approach of viable cell counts, 16S rRNA gene analysis, microsensor profiling and biogeochemical methods. The occurrence of magnetotactic bacteria was restricted to a narrow sediment layer overlapping or closely below the maximum oxygen and nitrate penetration depth. Different species showed different preferences within vertical gradients, but the largest proportion (63–98%) of magnetotactic bacteria was detected within the suboxic zone. In one microcosm the community of magnetotactic bacteria was dominated by one species of a coccoid "*Alphaproteobacterium*", as detected by denaturing gradient gel electrophoresis in sediment horizons from 1 to 10 mm depth. Maximum numbers of magnetotactic bacteria were up to 1.5×10^7 cells/cm^3, which corresponded to 1% of the total cell number in the upper sediment layer. The occurrence of magnetotactic bacteria coincided with the availability of significant amounts (6–60 μM) of soluble Fe(II), and in one sample with hydrogen sulfide (up to 40 μM). Although various trends were clearly observed, a strict correlation between the distribution of magnetotactic bacteria and individual geochemical parameters was absent. This is discussed in terms of metabolic adaptation of various strains of magnetotactic bacteria to stratified sediments and diversity of the magnetotactic bacterial communities.

Keywords: Magnetotactic bacteria; Vertical distribution; Chemical gradient; Freshwater sediment; Microsensors

1. Introduction

Magnetotactic bacteria (MTB) are aquatic microorganisms whose swimming direction is influenced by magnetic fields [1]. The ability of magnetotaxis is based on magnetosomes, which are intracellular membrane-bound crystals of a magnetic iron mineral, such as magnetite or greigite [2,3]. The function of magnetotaxis is generally assumed to facilitate the bacteria finding and maintaining a favorable position in vertical chemical gradients in stratified environments [1,4], although it has not been fully explored how exactly this position is correlated to geochemical parameters. Despite the ubiquitous and abundant occurrence of diverse magnetotactic bacteria in many marine and freshwater habitats, only a small number of magnetotactic strains could be isolated in pure culture so far (for review see [2]). Although they provide valuable models for laboratory investigation, insights into their metabolism, magnetosome biomineralization, and ecophysiology may not necessarily be generalized for the vast natural diversity of magnetotactic bacteria, as the known cultivated species do not represent the dominant species in their natural environment [5,6]. Further investigations of

* Corresponding author. Tel.: +49 421 2028 746; fax: +49 421 2028 580.

E-mail address: dschuele@mpi-bremen.de (D. Schüler).

0168-6496/$22.00
doi:10.1016/j.femsec.2004.11.006

uncultivated magnetotactic bacteria are thus required. A variety of diverse MTB can be easily enriched without cultivation by taking advantage of their magnetically directed swimming behavior [7,8]. This has enabled us to explore the morphological and phylogenetic diversity of uncultivated magnetotactic bacteria in many studies (for review see [6,9]). However, much less is known about their ecology and distribution in sediments and stratified water columns.

In an early report, the distribution of magnetotactic bacteria in the permanently stratified water column of the Pettaquamscutt River Estuary (USA) was addressed [10]. Whereas magnetotactic cocci could be detected only in the oxic and microoxic zone, diverse morphotypes were abundant (up to 2×10^5 cells/cm^3) not only in the microoxic but also in the anoxic zone in the presence of up to 2 mM sulfide. It was therefore concluded that the distribution of different magnetotactic bacteria is determined by different optima in sulfide and oxygen gradients. Another study investigated the vertical distribution of magnetite- and greigite-producing MTB in the same habitat [11]. Generally, more magnetite producers were found at and above the oxic–anoxic transition zone (OATZ), whereas more greigite-producing magnetotactic bacteria were located in the anoxic sulfidic zone. Similar observations were reported for a stratified water column of a brackish water pond [12]. Magnetotactic bacteria were observed only in the upper 10 cm of South-Atlantic deep-sea sediments, while none were detected in the water column [13]. Because the majority of magnetotactic bacteria in this study were found in the anoxic zone, where nitrate was available, it was suggested that most MTB might reduce nitrate as the terminal electron acceptor.

The spatial distribution of an uncultivated giant MTB species (''Magnetobacterium bavaricum'') from a freshwater habitat (Lake Chiemsee) was analyzed by fluorescence in situ hybridization (FISH) [5]. In microcosm experiments the occurrence of ''M. bavaricum'' was restricted to the sediment. Most cells were present within the microoxic zone with a peak abundance of 7×10^5 cells/cm^3 equivalent to a relative abundance of $0.64 \pm 0.17\%$. Because of its unusual large size, ''M. bavaricum'' accounted for approximately 30% of the biovolume within a narrow layer of the sediment, which indicates that magnetotactic bacteria may play a dominant role in the microbial ecology of the sediment.

Although these studies have indicated that magnetotactic bacteria are major constituents of microbial communities in certain zones of aquatic habitats, the biogeochemical interactions controlling their occurrence in stratified sediments have remained poorly understood. In this study, we therefore investigated the vertical distribution of magnetotactic bacteria in several freshwater microcosms. Because of the inavailability of a group-specific probe for the universal detection of magnetotactic bacteria by FISH, we used viable counts and denaturing gradient gel electrophoresis (DGGE) analyses to identify magnetotactic bacteria in sediments. The purpose of our experiments was to correlate the occurrence of magnetotactic bacteria in different sediment layers to data obtained by simultaneous characterization of the chemical microenvironments using microsensor profiling, direct activity measurements of sulfate reduction and further biogeochemical methods.

2. Material and methods

2.1. Sampling and setup of microcosms

Sediment samples from the upper sediment layer and surface water were collected from several marine and freshwater habitats in Northern Germany. Microcosms were set up essentially as described earlier [14] in bottles (0.1–2 l) or aquaria (5 l) for larger sample volumes. Briefly, approximately two thirds of sediment was overlaid with one third of sample water. The loosely covered containers were incubated at room temperature in dim light without agitation. Microcosms were stored in complete dark to prevent photosynthesis for 5 days before analysis. Because of their high cell numbers of MTB, four microcosms from three different freshwater habitats were selected for comprehensive analysis, which had been previously incubated for 30 (A), 17 (B), 17 (C) or 6 (D) months, respectively, and originated from the following freshwater sampling sites: (A) drainage ditch in Bremen, (B, C) eutrophic pond in Staßfurt (Sachsen-Anhalt), (D) a lake in Bremen (''Waller See''). Staßfurt samples (B and C) were collected from the same site, but at different times (B: April 2001, C: October 2001). Microcosm A and D were collected in March 2000 and April 2003, respectively. Cores from microcosms A and B (9 mm in diameter) were incubated for 5 days before analysis to reestablish physico-chemical gradients. Wider cores (26 mm in diameter) were taken from microcosms C and D for more detailed analysis. To avoid compression of sediment cores that may lead to disturbation of chemical gradients, a moderate vacuum was applied to these cores during the sampling.

2.2. Viable counts and DAPI counts

One sediment core per microcosm was sliced into 1–13 mm increments. The sediment samples were immediately diluted with sterile habitat water (1:2) and homogenized. For enumeration, 3 μl of sediment slurry was placed as a hanging drop onto a microscopic slide [15]. Counting was performed using a Zeiss (Jena, Germany)

Axioplan phase contrast microscope at 400× magnification. Aliquots were diluted appropriately with sterilized habitat water, so that 50–300 MTB per drop could be counted. Cells with a characteristic motility and magnetic response, which accumulated at the edge facing the magnetic south pole of a bar magnet, were considered as magnetotactic. Counting was started when virtually all magnetotactic bacteria had reached the edge, which was typically after 10–12 min. Average MTB numbers were calculated from three different drops. To investigate the influence of atmospheric oxygen onto the migration of magnetotactic bacteria, a control sample was analyzed in parallel under oxygen-containing and oxygen-free atmospheres. Since both samples yielded nearly identical MTB numbers, the effect of oxygen was considered negligible and all counts were subsequently performed in the presence of air.

For DAPI counts, the samples were fixed with paraformaldehyde, washed, subjected to sonification and filtered onto polycarbonate filters (pore size 0.2 μm, Millipore) as described by Pernthaler et al. [16]. The cells were stained with 4′,6′-diamidino-2-phenylindole (DAPI, Sigma, Schellendorf, Germany) for 4 min and washed with H_2O and 70% ethanol. After the embedding in Citifluor (Citifluor Products, Canterbury, UK) total cell numbers were counted using a Zeiss Axioplan fluorescence microscope. Mean cell numbers were calculated from several randomly chosen fields on each filter, corresponding to a minimum of 1000 DAPI-stained cells.

2.3. Electron microscopy

MTB from different sediment horizons were collected by a magnet as described above and adsorbed onto 300-mesh formvar coated copper grids (Plano, Wetzlar, Germany), which were examinated without staining with an EM 301 transmission electron microscope (Philips; Eindhoven, Netherlands) at 80 kV.

3. Magnetic collection of cells for PCR

To strictly separate MTB from particles and contaminants, 50 μl of each horizon (either directly or after 1:2 dilution with sterile habitat water) was applied to a special separation chamber that was build from two cellulose stripes, which were separating the sediment slurry from a reservoir of sterile habitat water under a cover slip. By application of a magnetic field, magnetotactic bacteria were directed by swimming through the cellulose stripes from the slurry into the reservoir, from where the separated cells were collected after 45 min. After concentration by centrifugation cells were resuspended in 11 μl water. Alternatively, magnetotactic bacteria were collected from microcosms by attaching the south pole of a bar magnet outside the bottle 1 cm above the sediment surface.

3.1. PCR amplification

Bacterial 16S rRNA genes from the resuspended cells were amplified with the universal primer pair GM5F with a GC-clamp and 907R [17]. The PCR system from TaKaRa Bio Incorporation (Otsu, Shiga 520-2193, Japan) was used according to manufacturer's instructions. The touchdown PCR was initiated by one cycle at an annealing temperature of 65 °C, which was gradually decreased by 1 °C in every other cycle down to 55 °C. For cloning, nearly complete 16S rRNA genes were amplified using the same PCR system with the universal bacterial primer pair GM3F and GM4R [17]. PCR was performed by 33 cycles at an annealing temperature of 42 °C. The PCR product was cloned into the pCR®4-TOPO® vector and transformed into competent *Escherichia coli* cells (TOP10) from Invitrogen (Carlsbad, USA). The plasmid DNA from positive clones was isolated with a QIAprep Spin Miniprep Kit (Quiagen, Hilden, Germany) and sequenced with GM1 (5′-CCAGCAGCCGCGGTAAT-3′) and vector-specific primers.

3.2. Denaturing gradient gel electrophoresis (DGGE)

DGGE was performed using the D-Gene™ system (Bio-Rad Laboratories, Munich, Germany) as described previously [18]. DNA fragments were separated in a 1-mm thick polyacrylamide gel (6% wt/vol) with a 20–70% denaturant gradient and 1 × TAE electrophoresis buffer (40 mM Tris, 20 mM acetic acid, 1 mM EDTA, pH 8.3) at 60 °C. After 16 h electrophoresis at a constant voltage of 100 V, the gel was stained with ethidium bromide and documented by the Image Master from Amersham Pharmacia. DNA bands were excised and eluted in 100 μl water overnight at 4 °C. About 1–6 μl of the eluates were reamplified with GM5F and 907R and PCR products were purified using the gel extraction kit (Eppendorf, Hamburg, Germany) from agarose gels and subsequently sequenced.

3.3. Sequence analysis

Purified PCR products or plasmid DNA (100 ng) were used in the sequencing reaction. DNA sequences were determined by a capillary sequencer (Applied Biosystems/Hitachi 3100 Genetic Analyzer, Foster City, Canada) and compared against databases using the BLAST algorithm (http://www.ncbi.nlm.nih.gov/BLAST/). The nucleotide sequences of partial 16S rRNA genes of magnetotactic bacteria have been deposited in the GenBank, EMBL, and DDJB libraries with Accession No. AJ863135 (microcosm D), AJ863150 (microcosm B) and AJ863158 (microcosm A).

3.4. Microsensor measurements

Concentration profiles of oxygen, sulfide, nitrate and pH were measured using custom-build microsensors. Amperometric Clark type sensors were applied for oxygen and sulfide determinations, potentiometric glass sensors for pH, while biosensors were used for determination of nitrate profiles. The diameter of the sensors was 10 μm (oxygen, pH, and sulfide) or 30 μm (nitrate). See [19] for detailed description and working principle of used microsensors. To ensure temporary and lateral homogeneity, chemical profiles were measured repeatedly before sampling. If not indicated otherwise (e.g., Fig. 1), all measurements yielded nearly identical results.

3.5. Geochemical analysis

Sediment cores were sliced under a nitrogen atmosphere into 0.5–2 cm sections and pore water was immediately separated from the sediments by centrifugation through 0.45 μm membrane filters. The water content of sediment samples was determined gravimetrically after drying at 104 °C for 24 h. Dissolved iron was measured spectrophotometrically by adding reducing ferrozine immediately after filtration (Ferrozine reagent with 1% hydroxylamine-hydrochloride) to the pore water [20]. To discriminate between the Fe(II) and Fe(III) ions, the reducing agent was added to the ferrozine assay after a previous measurement in which hydroxylamine-hydrochloride was omitted [20]. In addition, high resolution measurements of dissolved iron and manganese in the pore water were performed using the technique of diffusive equilibration in thin films (DET; [21,22]). In this technique solutes equilibrate with the water of the hydrogels, which are removed from the sediment after 24 h and subsequently sliced and reequilibrated for 24 h with HNO_3 (2% s.p). Dissolved iron and manganese concentrations were analyzed by optical emission spectroscopy (ICP, Perkin–Elmer Optima 3000XL) using scandium as an internal standard.

Extractable iron includes fractions of iron (III) in sediments, which is available for chemical reduction and readily reacts with sulfide to form various iron sulfide minerals and eventually pyrite [23]. The proportion of extractable iron was quantified by the Ferrozine method (see above) after extraction for 1 h at room temperature with either buffered Na-dithionite solution [23] or 0.5 M HCl [24]. While the HCl-extraction reveals the amount of ferrihydrites and iron monosulfides, leachable iron extracted by dithionite represents both poorly and well-crystallized iron oxides, e.g., hematite, and minor iron bond to silicates [23,24]. Both extraction methods showed nearly similar results therefore only data from dithionite extraction are presented in the results.

Sulfate concentrations in the pore water were determined by ion chromatography (Waters). Microbial sulfate reduction rates were measured using the whole core incubation method. The sediment core (26 mm in diameter) was injected with a carrier-free $^{35}SO_4^{2-}$ tracer and incubated for 4 h at room temperature. Tracer recovery after microbial conversion was measured for both the fraction of acid-volatile sulfide (AVS, essentially FeS) and chromium-reducible sulfur (CRS, essentially elemental sulfur) by the two step distillation method [25,26]. Total gross sulfate reduction rate (SRR) is the sum of both fractions. The spatial distribution of bacterial sulfate-reducing activity was visualized by the application of the in situ 2D-photopaper monitoring technique, which is a modification of a method described in [27], and is based on the diffusion of hydro-

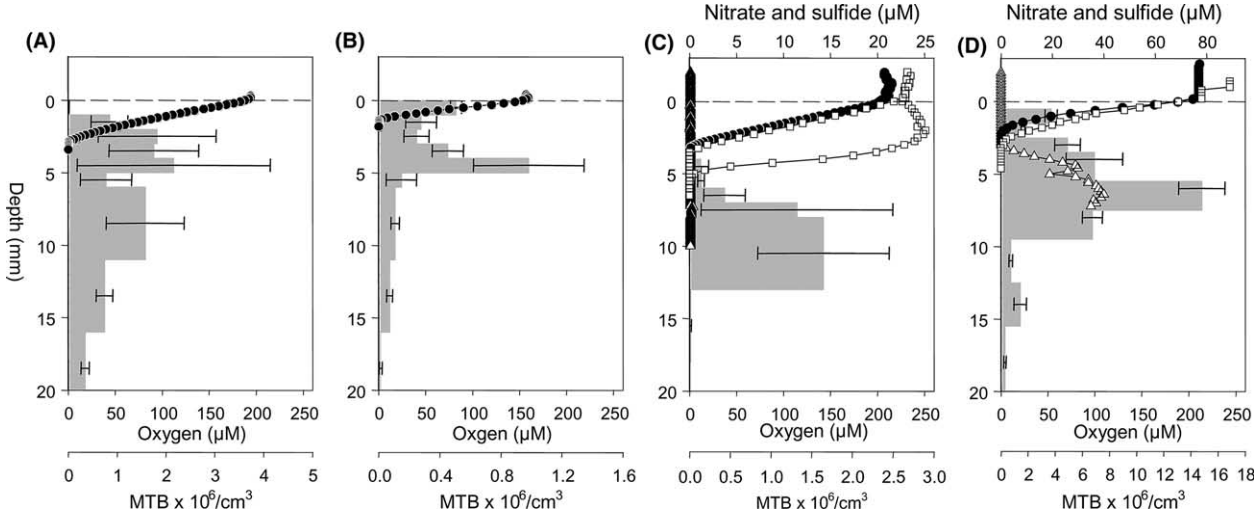

Fig. 1. Vertical distributions of magnetotactic bacteria in microcosms A, B, C and D in relation to downcore profiles of: oxygen (●), nitrate (□), and sulfide (△) concentrations. Numbers of magnetotactic bacteria (MTB) are shown as grey vertical bars with standard deviations indicated. Sediment surface is indicated as a dashed line. Two different nitrate curves were obtained from measurements at two different sites within the microcosm C.

gen sulfide into a photographic paper with subsequent Ag_2S formation. Photographic paper was incubated for 23–25 h followed by the fixation in a 2 M sodium thiosulfate solution.

To establish the nature of mineral phases of the solid phases that precipitated at the walls of the incubation vessels, FTIRspectroscopy (Mattson 3000 type FTIR spectrophotometer) and X-ray powder diffraction (Philips X-ray powder diffractometer) were used. Pore water profiles were additionally interpreted by the modeling program PROFILE [28] to calculate net rates of production or consumption as a function of depth.

4. Results

4.1. Development of microcosms

Typically, various characteristic morphotypes of magnetotactic bacteria including cocci, spirilla, rods and vibrios were present in most fresh samples. Both marine and freshwater microcosms underwent a characteristic succession within several weeks. Marine samples generally contained low numbers of MTB, which rapidly disappeared upon laboratory incubation. Generally, the total MTB numbers increased in most freshwater microcosms within several weeks. This was coincident with an apparent loss of diversity, and most microcosms were ultimately dominated by few morphotypes after prolonged incubation. In those samples, MTB populations remained apparently stable for periods of up to several years without obvious changes in cell numbers and morphologies. Therefore, four of these aged microcosms (A, B, C, D) from three different freshwater habitats were selected for further examination of distribution of magnetotactic bacteria.

4.2. Biogeochemical characteristics of microcosms

The succession in the MTB population coincided with a noticeable change in the appearance of microcosms. A characteristic stratification of the sediments became visible after several weeks of incubation, which reflected changes in the biogeochemical processes. The upper sediment layer of microcosm C had a silty appearance, while coarse-grained sediment prevailed below depth of about 18 mm. Surface sediments showed indications for bioturbation. The brownish sediment turned black below about 10 mm due to the reduction of Fe(III) minerals and the precipitation of iron monosulfides. The presence of FeS was proven by the smell of H_2S after liberation from the sediment upon attack with diluted hydrochloric acid. Below about 30 mm depth the sediment turned grey due to the formation of pyrite and it contained gas bubbles (presumably methane), besides plant residues. Water contents reached about 75% at the surface that decreased to below 30% in the coarse-grained bottom part. Microcosm D, containing more sandy sediment, displayed stratification marked by color change. The light-brownish-gray oxic surface extended over 3 mm and turned into a darker layer down to 30 mm depth. The following grey-colored section of the sediment was laminated with two distinct darker layers at about 40 and 50 mm depth.

During the time of sampling, maximum oxygen penetration depth varied between the four microcosms (A: 2.5 mm; B: 1.5 mm; C: 3.0 mm; D: 2.0 mm; Fig. 1), but displayed only slight variations (less than 0.5 mm) within a single setup. In microcosms C and D additional profiles of nitrate, sulfide and pH were obtained. In both microcosms nitrate was measurable and maximum penetration depth was generally 0.5 mm deeper than oxygen (Figs. 1C and D). However, at one particular spot in microcosm C, a deeper maximum penetration depth of nitrate was observed (5.0 mm), which was possibly due to locally enhanced nitrification rates (Fig. 1C). Although photopaper-monitoring techniques indicated the occurrence of dissolved sulfide in microcosm C (data not shown), no free sulfide (H_2S) was measurable by microsensors, probably due to the rapid reoxidation at the surface (Fig. 1C). In microcosm D hydrogen sulfide could be detected below the depth of 3.0 mm. Interestingly, dissolved sulfide did not overlap with either oxygen or nitrate (Fig. 1D). Values of pH decreased from 8.5 at the sediment surface to 7.0 in deeper sediment layers in microcosm C, but remained stable at 6.7 in the sediment of microcosm D (data not shown).

Maximum sulfate concentrations in the surface waters of microcosms C and D were 4 mM and 1.4 mM, respectively, and decreased downcore (Fig. 2). Modeling with PROFILE revealed a distinct zone of sulfate consumption in the upper 4 cm of microcosm C (data not shown). This result was further substantiated by the direct measurements of gross sulfate reduction rates (SRR). Gross SRR were found throughout the investigated sediment sections with maxima at about 4.5 cm depth (Fig. 2). The surface values of sulfate reduction rates of 10 nmol/cm^3/d increased up to maximum rates of 70 nmol/cm^3/d at 4.5 cm depth with a subsequent decline. Effected by reoxidation, sulfate reduction rates showed net production of AVS during short-time incubation just below 1.5 cm depth and reached maximum values at 4.5 cm depth. In microcosm D modeling with PROFILE did reveal sulfate depletion below the maximum of SRR at approximately 2.5 cm depth (data not shown). The rates were about 20 times higher compared to microcosm C. AVS started to accumulate just below 1.5 cm depth, indicating effective reoxidation in the top part of the sediment (Fig. 2).

In microcosm C an increase of Fe(II) was detected below 0.5 cm depth and reached up to 110 μM at 2

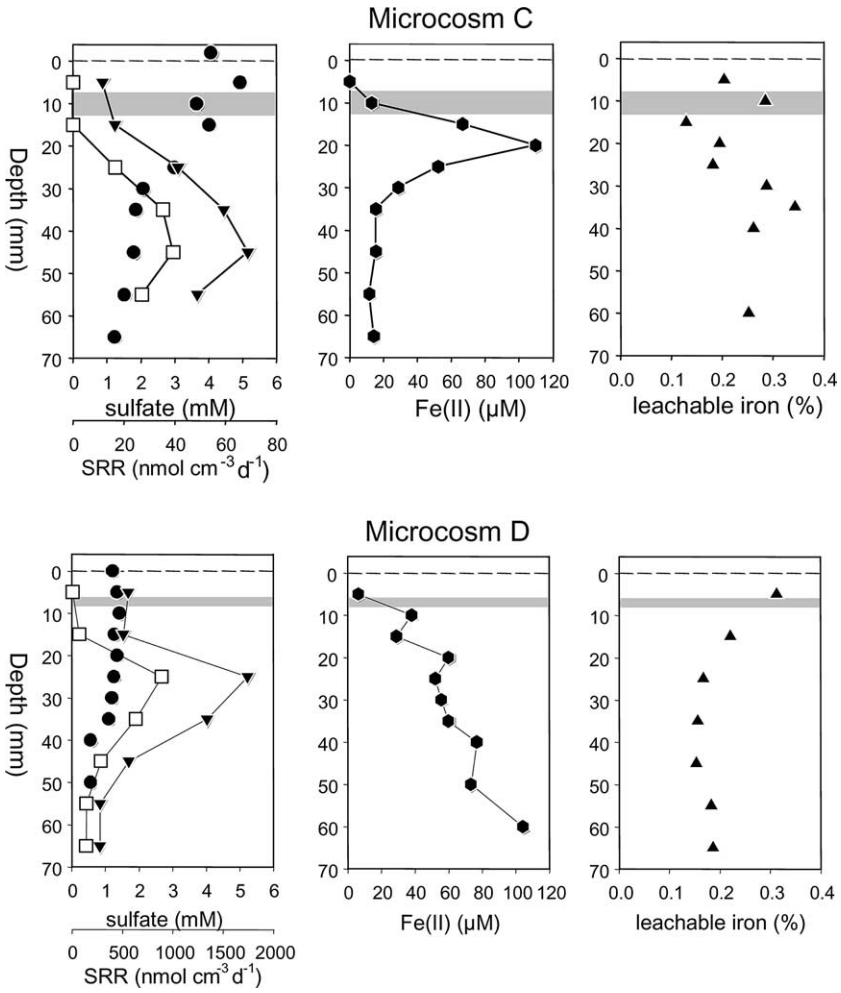

Fig. 2. Vertical distributions of magnetotactic bacteria in microcosms C and D in relation to downcore profiles of sulfate concentrations (●), gross (▼) and AVS (□) sulfate reduction rates, dissolved (⬟) and leachable (▲) iron. Horizons with maximum abundances of magnetotactic bacteria are indicated as grey vertical bars. Sediment surface is indicated as a dashed line.

cm depth (Fig. 2). In deeper sections, iron monosulfide was present contributing to the fraction extracted by Na-dithionite and leading also to a decrease in dissolved Fe(II) concentrations. For the upper sediment zone a net iron reduction rate of 17 nmol/cm^3/d was calculated (data not shown). Dissolved iron was released into the pore water below the oxygen penetration depth of about 5 mm up to 104 μM in microcosm D (Fig. 2). The depth profile of leachable iron indicates a depletion of Fe(III) below the first cm due to chemical reduction by sulfide in agreement with the accumulation of dissolved Fe(II) (Fig. 2). The combined results of SRR and Fe(III) reduction rates indicate that this is a zone where both chemical and microbial iron reduction takes place in both microcosms. The precipitation of ferrihydrites and manganese dioxides at the walls of microcosm D indicated that near surface metal reduction led at least temporary to the liberation of dissolved iron and manganese to the overlying water, where reoxidation took place.

4.3. Vertical distribution of magnetotactic bacteria

Analysis of viable cell numbers revealed a heterogeneous vertical distribution of magnetotactic bacteria in all microcosms. No magnetotactic bacteria were detectable in the oxic water columns and their occurrence was restricted to a narrow layer in the sediment, which was overlapping or closely below the OATZ. However, different microcosms displayed variations in the abundance and distributions of MTB.

In microcosm A highest numbers of MTB (2.3×10^6 cells/cm^3) were present between 4 and 5 mm depth (Fig. 1A). No other morphotypes than magnetotactic cocci were observed by microscopy. In contrast, two maxima of distribution were found in microcosm B (Fig. 1B). The first maximum of 5.1×10^5 MTB/cm^3 was found immediately below the surface in the microoxic sediment zone and consisted of different morphotypes including magnetotactic cocci and spirilla. A second peak (9.7×10^5 MTB/cm^3) occurred in the anoxic

zone between 4 and 5 mm depth and consisted exclusively of magnetotactic cocci.

Likewise, a heterogeneous distribution of different morphotypes was observed in microcosm C. Beside the presence of cocci, this microcosm was dominated by magnetotactic spirilla. Unlike magnetotactic cocci, spirilla performed a bidirectional swimming motility [4], but nevertheless displayed a north-seeking net polarity. Both cocci and spirilla were present in the oxic as well as in the anoxic zone of the sediment, but were most abundant between 8 and 13 mm depth (1.6×10^6 MTB/cm^3, Fig. 1C; proportion of cocci was 8.0%, data not shown). Interestingly, this peak did partially overlap the presence of soluble ferrous iron of 25–60 μM (Fig. 2). The number of magnetotactic bacteria steeply declined in deeper sediment layers.

In microcosm D, MTB could be detected in all horizons down to 45 mm. A single maximum of 14.8×10^6 MTB/cm^3 was detectable in the anoxic sediment between 6 and 8 mm depth where 6–40 μM Fe(II) is available (Figs. 1D and 2). Total cell numbers in this layer were determined by the DAPI method and were 10^9 cells per cm^3. Thus, magnetotactic bacteria accounted for approximately 1% of the total microbial population of this particular horizon. In contrast to magnetotactic cocci, which were most abundant at this depth (14.6×10^6 cells/cm^3), magnetotactic spirilla occurred in highest numbers (0.5×10^6 cells/cm^3) in the upper anoxic layer between 4 and 6 mm depth, but were absent from deeper sediment layers (Fig. 3A).

4.4. Morphological and phylogenetic diversity of magnetotactic bacteria from different horizons

Microscopic analysis indicated that the MTB distribution in our microcosms was heterogeneous not only with respect to cell numbers, but also to the composition of the magnetotactic population (Figs. 3C, D). Differences were observed between different sediment layers of a single microcosm as well as between microcosms from different sampling sites, as indicated by microscopy and 16S rRNA gene analysis of MTB, which were magnetically collected without depth fractionation. While for instance a sequence from microcosm A revealed high similarity to the uncultivated magnetotactic coccus maccs13 (CS103, Accession No. X61605), a sequence from microcosm B affiliated with a different uncultivated magnetotactic bacteria (Accession No. AJ223476).

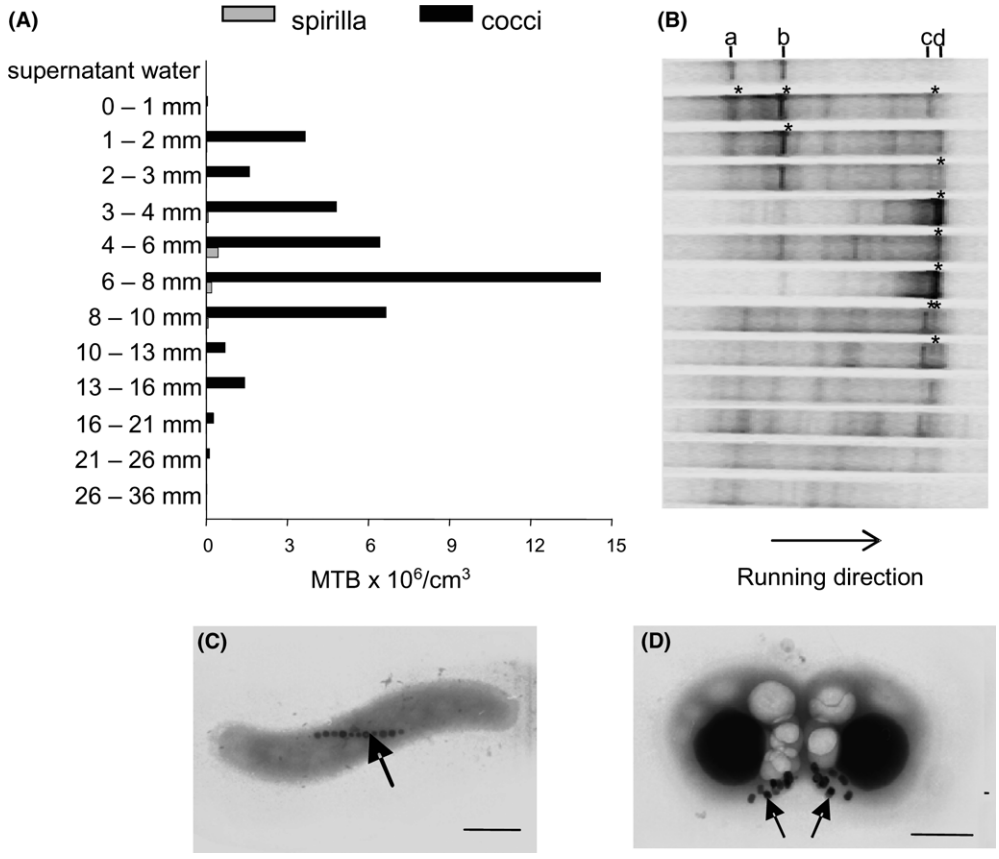

Fig. 3. (A) Vertical abundances of different morphotypes of magnetotactic bacteria in microcosm D. (B) DGGE band patterns obtained with primers GM5F + GC-clamp and 907R from cells that were magnetically purified from different horizons of microcosm D. The marked bands (*) were excised and sequenced. (C, D) Electron micrographs of different magnetotactic bacteria, which were characteristic for microcosm D. Arrows indicate magnetosome particles (bar = 0.5 μm).

To investigate the vertical distribution of different species, magnetotactic bacteria were collected from different sediment layers of microcosm D. Fig. 3B shows the results of the DGGE of PCR-amplified 16S rRNA gene fragments obtained from the water column and magnetically enriched cells from different sediment layers. Two major bands (a and b) were obtained from the water column. These bands were also present in the upper zone of the sediment, but their intensity decreased in deeper sediment layers. Sequences obtained from a and b displayed highest similarity to those from the *Cytophaga Flavobacterium Bacteroides* cluster, while a third band (c) from the upper and deeper sediment layers yielded a sequence closely related to *Pseudomonas spinosa*. A further distinct band (d) was abundant in DGGE patterns from 1 to 10 mm depth, which was coincident with the maximum abundance of magnetotactic bacteria. Sequencing of this band confirmed its identity in all horizons and revealed high sequence similarity to a sequence from an uncultivated magnetic coccus in the database (Accession No. X80996). To obtain extended sequence information, the nearly complete 16S rRNA gene was amplified from cells collected from 6 to 8 mm depth, the horizon that had revealed only one dominant band in DGGE. One sequence was obtained, which matched the partial sequences from b and d in the DGGE profile and displayed only four mismatches to the uncultivated magnetococcus [29]. Hence, the DGGE profiles from different sediment layers confirmed the heterogeneous vertical distribution of magnetotactic bacteria and were consistent with the distribution of total viable MTB numbers. However, molecular analysis did not fully reveal the diversity of magnetotactic bacteria observed by microscopy during cell counts and electron microscopy. Microscopy of the magnetotactic cells collected for PCR revealed that in contrast to direct counts in the hanging drop, only magnetotactic cocci were observed in significant numbers. This might be a consequence of the more stringent collection conditions employed for PCR amplification, which had resulted in the loss of other magnetotactic bacterial species (e.g., spirilla) below detection.

5. Discussion

Viable counts of magnetotactic bacteria possibly slightly underestimate the abundance of these bacteria, because the method is intrinsically biased for highly motile cells, while slow-moving bacteria or cells that were attached to sediment particles are possibly missed. Nevertheless, counts of magnetically separated cells have proven an effective and highly selective tool for the enumeration of magnetotactic bacteria in this study. All of our selected samples were characterized by the development of abundant populations of magnetotactic bacteria, however, these varied considerably in numbers and community compositions between different microcosms. The observed downcore profiles of microbial activity and dissolved constituents confirmed the presence of steep opposing gradients of reduced and oxidized compounds in the surface sediment of the investigated microcosms. In all samples this coincided with the occurrence of magnetotactic bacteria, which was restricted to a narrow layer in the upper sediment located closely to the OATZ. As most of the cultivated MTB strains are known to behave as typical microaerophiles, it was surprising that in all microcosms most magnetotactic bacteria were detected in the suboxic zone immediately below the OATZ (A: 63%, B: 92%, C: 98% and D: 91%). Maximum numbers were between 9.7×10^5 and 1.5×10^7/cm^3, thus accounting for at least 1% of the total cell numbers in this region. Interestingly, in microcosm B magnetic spirilla were more abundant in microoxic sediment layers, whereas magnetic cocci were predominantly found in the deeper suboxic zone, indicating that different species showed different preferences within the vertical gradients. The maximum MTB numbers in our study were considerably higher than MTB numbers estimated for environmental samples (10^3–10^4 MTB/cm^3, [14,30]), but were in the same range as reported previously for other laboratory enrichments [5,14,31,32].

Although all magnetotactic bacteria apparently displayed a very strict preference within the vertical chemical zonation, e.g., the restriction to a very narrow layer, the pathway of electron transfer and their putative mode of metabolism are not apparent from the distribution of potential electron donors and acceptors investigated. Cultivated magnetotactic bacteria are metabolically versatile and all investigated species are known to perform a strictly respiratory metabolism, which can be coupled to the oxidation of organic substrates, such as short-chained fatty acids. We did not measure organic compounds, but studies on other stratified environments, i.e., a microbial mat, showed that the occurrence of these typical fermentation products was restricted to the upper layers slightly below the oxic zone [33]. Analogous, the peak abundance of magnetotactic bacteria in our microcosms thus might reflect the availability of these organic carbon sources.

In addition, the availability of inorganic electron donors must be considered as an important factor controlling the distribution of magnetotactic bacteria. Several isolated MTB strains are able to grow by the oxidation of sulfide in opposing sulfide-oxygen gradients [34,35]. *Sox* genes, which encode enzymes essential for the oxidation of reduced sulfur compounds [36] are present in the genomes of various *Magnetospirillum* species (DOE Joint Genome Institute www.jgi.doe.gov/JGI_microbial/html; Flies and Schüler, unpublished), suggesting that the ability to oxidize reduced sulfur compounds is ubiquitous among MTB. In MV-1, evidence for a facultative autotrophic metabolism based on the oxidation of

sulfide or thiosulfate was found [35]. The majority of the magnetotactic bacteria found in our microcosms contained inclusions, which probably represented sulfur globules similar as reported in numerous uncultivated magnetotactic bacteria from freshwater and marine habitats [5,35,37–40]. Intracellular sulfur globules are commonly found in other bacteria as metabolic products of H_2S oxidation. Sulfide could be detected in microcosm D and sulfur intermediates (as S°) coincided with the occurrence of magnetotactic bacteria in this microcosm. In microcosm C monitoring by photopaper also demonstrated the presence of dissolved sulfide in sediment layers where magnetotactic bacteria were found. Thus, the assumption of a sulfide-oxidizing metabolism would be reasonable for the MTB populations in microcosm C and D.

Whereas sulphate-reducing bacteria (SRB) seem to be important in the shaping of gradients in the investigated sediments, no magnetotactic bacteria could be detected at the depth of maximum sulfate reduction. With the exception of *Desulfovibrio magneticus* from the "*Deltaproteobacteria*", all cultivated magnetotactic bacteria are unable of sulfate reduction. Indeed, the most abundant magnetotactic bacteria in microcosm D were identified as "*Alphaproteobacteria*", which are unlikely to respire sulfate. Thus, sulfate reduction is probably not a major metabolic pathway in most magnetotactic bacteria from freshwater.

Several previous reports have implicated magnetotactic bacteria in the reduction of iron and it has been suggested that they potentially derive energy from this process [41–43]. In our experiments, magnetotactic bacteria were found in a zone where abundant solid phase Fe(III) was present and thus, potentially might serve as an electron acceptor. However, there are no clear experimental indications that dissimilatory iron reduction is a metabolic pathway in cultivated magnetotactic bacteria, and its relevance for populations in our microcosm remains uncertain. However, besides its putative function in redox cycling, iron plays an eminent role in magnetotactic bacteria, since large amounts of iron are required for the synthesis of magnetosome crystals that account for 2–4% of the dry weight [14,44]. Intriguingly, the abundance of magnetotactic bacteria in our microcosms coincided with the availability of dissolved iron in the top surface sediments. Ferrous iron concentrations in the pore water of these sediment layers are in the range, which are saturating for both growth and magnetosome formation in cultures of *Magnetospirillum gryphiswaldense* and other magnetotactic bacteria [44–46]. Thus, the availability of iron for the synthesis of magnetosomes appears to be another factor affecting the distribution of magnetotactic bacteria.

With the exception of *D. magneticus*, all cultivated MTB strains can use molecular oxygen and nitrous compounds (i.e., nitrate or nitrous oxide) as terminal electron acceptors for respiration ([14,47–52]; Heyen and Schüler, unpublished). However, contrary to our expectations the occurrence of magnetotactic bacteria in our microcosms was not coincident with the presence of either nitrate or oxygen. The position of magnetotactic bacteria within multiple gradients of dissolved species might not be strictly determined by a single factor, but may rather represent a "trade-off" between the availability of electron donors and acceptors as well as iron. This potentially may involve temporary displacements between different zones, and energy taxis in combination with magnetic orientation may play an important role in the control of vertical distribution in MTB. One possible mode of metabolism would be that magnetotactic bacteria shuttle electrons by migration between zones of sulfide oxidation and oxygen or nitrate reduction. However, due to their small size the observed magnetotactic bacteria are unlikely to store significant amounts of an electron acceptor for the provision of energy during migration, such as for instance nitrate-storing sulfide-oxidizing *Thioploca* and *Beggiatoa* species do [53,54]. Thus, the predominant occurrence of magnetotactic bacteria in zones lacking an appropriate electron acceptor remains somewhat puzzling. Unless there is a so-far unknown capability of magnetotactic bacteria to derive energy by fermentation or respiration on different electron acceptors, for instance such as humic acids, their preferred occurrence closely to, but outside of oxic zones in our aged microcosms might alternatively reflect a resting or metabolically inactive state, which is occupied in the absence of higher concentrations of organic substrates. This would be consistent with the stunning observation that viable magnetotactic bacteria can be recovered in high numbers from sediment micro- and mesocosms even after many years of incubation in the dark without any addition of a carbon or energy source ([1]; Flies, unpublished observation). Thus, our aged microcosms may not generally reflect environmental conditions, as conditions in natural sediments are likely to be more dynamic due to the continuous influx of organic substance and the impact of photosynthesis. Further studies, such as in situ measurements of metabolic activity of magnetotactic bacteria in undisturbed sediments from marine and freshwater habitats are therefore urgently required.

Acknowledgements

We thank P.-L. Gehlken, Heiligenstadt, for carrying out the FTIR and XRD measurements, F. Mayer and M. Hoppert, Göttingen, for providing access to the electron microscope, and A. Schipper for help in the laboratory. This work was supported by the BMBF and the Max Planck Society.

References

[1] Blakemore, R.P. (1975) Magnetotactic bacteria. Science 190 (4212), 377–379.

[2] Bazylinski, D.A. and Frankel, R.B. (2004) Magnetosome formation in prokaryotes. Nat. Rev. 2, 217–230.

[3] Schüler, D. (2004) Molecular analysis of a subcellular compartment: the magnetosome membrane in *Magnetospirillum gryphiswaldense*. Arch. Microbiol. 181, 1–7.

[4] Frankel, R.B., Bazylinski, D.A., Johnson, M.S. and Taylor, B.L. (1997) Magneto-aerotaxis in marine coccoid bacteria. Biophys. J. 73 (2), 994–1000.

[5] Spring, S., Amann, R., Ludwig, W., Schleifer, K.-H., Van Gemerden, H. and Petersen, N. (1993) Dominating role of an unusual magnetotactic bacterium in the microaerobic zone of a freshwater sediment. Appl. Environ. Microbiol. 59 (8), 2397–2403.

[6] Spring, S. and Schleifer, K.-H. (1995) Diversity of magnetotactic bacteria. Syst. Appl. Microbiol. 18, 147–153.

[7] Wolfe, R.S., Thauer, R.K. and Pfennig, N. (1987) A capillary racetrack method for isolation of magnetotactic bacteria. FEMS Microbiol. Ecol. 45 (1), 31–36.

[8] Schüler, D., Spring, S. and Bazylinski, D.A. (1999) Improved technique for the isolation of magnetotactic spirilla from a freshwater sediment and their phylogenetic characterization. Syst. Appl. Microbiol. 22 (3), 466–471.

[9] Amann, R., Rossello-Mora, R., Flies, C.B. and Schüler, D. (2004) Phylogeny and in situ identification of magnetotactic bacteria In: Biomineralization (Baeuerlein, E., Ed.). Wiley-VCH, Weinheim.

[10] Stolz, J.F. (1992) Magnetotactic bacteria: Biomineralization, ecology, sediment magnetism, environmental indicator In: Biomineralization: Processes of Iron and Manganese; Modern and Ancient Environments (Skinner, H.C.W., Ed.), pp. 133–145. Catena-Verlag, Cremlingen-Destedt.

[11] Bazylinski, D.A., Frankel, R.B., Heywood, B.R., Mann, S., King, J.W., Donaghay, P.L. and Hanson, A.K. (1995) Controlled biomineralization of magnetite (Fe_3O_4) and greigite (Fe_3S_4) in a magnetotactic bacterium. Appl. Environ. Microbiol. 61, 3232–3239.

[12] Bazylinski, D.A. and Moskowitz, B.M. (1997) Microbial biomineralization of magnetic iron minerals: Microbiology, magnetism and environmental significance In: Geomicrobiology: Interactions Between Microbes and Minerals, pp. 181–223. Catena-Verlag, Cremlingen-Destedt.

[13] Petermann, H. and Bleil, U. (1993) Detection of live magnetotactic bacteria in South-Atlantic deep-sea sediments. Earth Planet. Sci. Lett. 117 (1–2), 223–228.

[14] Blakemore, R.P., Maratea, D. and Wolfe, R.S. (1979) Isolation and pure culture of a freshwater magnetic spirillum in chemically defined medium. J. Bacteriol. 140, 720–729.

[15] Schüler, D. (2002) The biomineralization of magnetosomes in *Magnetospirillum gryphiswaldense*. Int. Microbiol. 5 (4), 209–214.

[16] Pernthaler, J., Glöckner, F.-O., Schönhuber, W. and Amann, R. (2001) Fluorescence in situ hybridization (FISH) with rRNA-targeted oligonucleotide probes In: Methods in Microbiology (Paul, J.H., Ed.), pp. 207–226. Academic press, San Diego.

[17] Muyzer, G., Teske, A. and Wirsen, C.O. (1995) Phylogenetic relationships of *Thiomicrospira* species and their identification in deep-sea hydrothermal vent samples by denaturing gradient gel electrophoresis of 16S rDNA fragments. Arch. Microbiol. 164, 165–172.

[18] Muyzer, G., Brinkhoff, T., Nübel, U., Santegoeds, C., Schäfer, H. and Wawer, C. (1998) Denaturing gradient gel electrophoresis (DGGE) in microbial ecology (Akkermans, A.D.L., van Elsas, F.J. and de Bruijn, F.J., Eds.), Molecular Microbial Ecology Manual, vol. 3.4.4, pp. 1–27. Kluwer Academic Publishers, Dordrecht.

[19] Kühl, M. and Revsbech, N.P. (1999) Microsensors for the study of interfacial biogeochemical processes In: The Benthic Boundary Layer (Boudreau, B.P. and Jørgensen, B.B., Eds.), pp. 180–210. Oxford University Press, Oxford.

[20] Viollier, E., Inglett, P., Hunter, K., Roychoudhury, A. and Van Cappellen, P. (2000) The ferrozine method revisited: Fe(II)/Fe(III) determination in natural waters. Appl. Geochem. 15 (6), 785–790.

[21] Davison, W. and Zhang, H. (1994) In-situ speciation measurements of trace components in natural-waters using thin-film gels. Nature 367 (6463), 546–548.

[22] Zhang, H. and Davison, W. (1999) Diffusional characteristics of hydrogels used in DGT and DET techniques. Anal. Chim. Acta 398 (2–3), 329–340.

[23] Canfield, D.E. (1989) Reactive iron in marine sediments. Geochim. Cosmochim. Acta 53, 619–632.

[24] Kostka, J.E. and Luther, G.W. (1994) Partitioning and speciation of solid-phase iron in salt-marsh sediments. Geochim. Cosmochim. Acta 58 (7), 1701–1710.

[25] Fossing, H. and Jørgensen, B.B. (1989) Measurement of bacterial sulfate reduction in sediments - evaluation of a single-step chromium reduction method. Biogeochemistry 8 (3), 205–222.

[26] Kallmeyer, J., Ferdelman, T., Weber, A., Fossing, H. and Jørgensen, B.B. (2004) A cold chromium distillation procedure for radiolabeled sulfide applied to sulfate reduction measurements. Limnol. Oceanogr. Methods 2, 171–180.

[27] Lehmann, C. and Bachofen, R. (1999) Images of concentrations of dissolved sulphide in the sediment of a lake and implications for internal sulphur cycling. Sedimentology 46, 537–544.

[28] Berg, P., Risgaard-Petersen, N. and Rysgaard, S. (1998) Interpretation of measured concentration profiles in sediment pore water. Limnol. Oceanogr. 43 (7), 1500–1510.

[29] Spring, S., Amann, R., Ludwig, W., Schleifer, K.-H., Schüler, D., Poralla, K. and Petersen, N. (1994) Phylogenetic analysis of uncultured magnetotactic bacteria from the Alpha-Subclass of Proteobacteria. Syst. Appl. Microbiol. 17 (4), 501–508.

[30] Blakemore, R.P. (1982) Magnetotactic bacteria. Annu. Rev. Microbiol. 36, 217–238.

[31] Moench, T.T. and Konetzka, W.A. (1978) A novel method for the isolation and study of a magnetotactic bacterium. Arch. Microbiol. 119, 203–212.

[32] Petersen, N., Weiss, D.G. and Vali, H. (1989) Magnetic bacteria in lake sediments In: Geomagnetism and Paleomagnetism (Lowes, F.J., et al., Eds.), pp. 231–241. Kluwer Academic Publishers, Dordrecht.

[33] Jonkers, H.M., Ludwig, R., De Wit, R., Pringault, O., Muyzer, G., Niemann, H., Finke and de Beer, D. (2003) Structural and functional analysis of microbial mat ecosystem from a unique permanent hypersaline inland lake: ''La Salada de Chiprana'' (NE Spain). FEMS Microbiol. Ecol. 44, 175–189.

[34] Meldrum, F.C., Mann, S., Heywood, B.R., Frankel, R.B. and Bazylinski, D.A. (1993) Electron microscopy study of magnetosomes in two cultured vibrioid magnetotactic bacteria. Proc. R. Soc. Lond. Ser. B 251 (1332), 237–242.

[35] Bazylinski, D.A., Dean, A.J., Williams, T.J., Long, L.K., Middleton, S.L. and Dubbels, B.L. (2004) Chemolithoautotrophy in the marine, magnetotactic bacterial strains MV-1 and MV-2. Arch. Microbiol. 182 (5), 373–387.

[36] Friedrich, C.G. (1998) Physiology and genetics of sulfur-oxidizing bacteria. Adv. Microb. Physiol. 39, 235–289.

[37] Moench, T.T. (1988) *Bilophococcus magnetotacticus* gen. nov. sp. nov., a motile, magnetic coccus. Anton. Leeuw. 54, 483–496.

[38] Iida, A. and Akai, J. (1996) Crystalline sulfur inclusions in magnetotactic bacteria. Sci. Rep. Niigata Univ. Ser. E (Geology) 11, 35–42.

[39] Bazylinski, D.A. and Frankel, R.B. (2000) Biologically controlled mineralization of magnetic iron minerals by magnetotactic bacteria In: Environmental Microbe–Metal Interactions (Lovley, D.R., Ed.), pp. 109–143. ASM Press, Washington, DC.
[40] Cox, L., Popa, R., Bazylinsky, D.A., Lanoil, B., Douglas, S., Belz, A., Engler, D. and Nealson, K.H. (2002) Organization and elemental analysis of P-, S-, Fe-rich inclusions in a population of freshwater magnetococci. Geomicrobiol. J. 19, 387–406.
[41] Guerin, W.F. and Blakemore, R.P. (1992) Redox cycling of iron supports growth and magnetite synthesis by *Aquaspirillum magnetotacticum*. Appl. Environ. Microbiol. 58 (4), 1102–1109.
[42] Paoletti, L.C. and Blakemore, R.P. (1988) Iron reduction by *Aquaspirillum magnetotacticum*. Curr. Microbiol. 17, 339–342.
[43] Short, K.A. and Blakemore, R.P. (1986) Iron respiration-driven proton translocation in aerobic bacteria. J. Bacteriol. 167 (2), 729–731.
[44] Schüler, D. and Baeuerlein, E. (1998) Dynamics of iron uptake and Fe_3O_4 biomineralization during aerobic and microaerobic growth of *Magnetospirillum gryphiswaldense*. J. Bacteriol. 180 (1), 159–162.
[45] Schüler, D. and Baeuerlein, E. (1996) Iron-limited growth and kinetics of iron uptake in *Magnetospirillum gryphiswaldense*. Arch. Microbiol. 166, 301–307.
[46] Heyen, U. and Schüler, D. (2003) Growth and magnetosome formation by microaerophilic *Magnetospirillum* strains in an oxygen-controlled fermentor. Appl. Microbiol. Biotechnol. 61 (5–6), 536–544.
[47] Blakemore, R.P., Short, K.A., Bazylinski, D.A., Rosenblatt, C. and Frankel, R.B. (1985) Microaerobic conditions are required for magnetite formation within *Aquaspirillum magnetotacticum*. Geomicrobiol. J. 4 (1), 53–72.
[48] Bazylinski, D.A., Frankel, R.B. and Jannasch, H.W. (1988) Anaerobic magnetite production by a marine magnetotactic bacterium. Nature 334 (6182), 518–519.
[49] Matsunaga, T., Sakaguchi, T. and Tadokoro, F. (1991) Magnetite formation by a magnetic bacterium capable of growing aerobically. Appl. Microbiol. Biotechnol. 35, 651–655.
[50] Meldrum, F.C., Mann, S., Heywood, B.R., Frankel, R.B. and Bazylinski, D.A. (1993) Electron microscopy study of magnetosomes in a cultured coccoid magnetotactic bacterium. Proc. R. Soc. Lond. Ser. B 251 (1332), 231–236.
[51] Kimble, L.K. and Bazylinski, D.A. (1996) Chemolithoautotrophy in the marine magnetotactic bacterium, strain MV-1. In: Annual Meeting of American Society Microbiology.
[52] Dean, A.J. and Bazylinski, D.A. (1999) Genome analysis of several marine, magnetotactic bacterial strains by pulsed-field gel electrophoresis. Curr. Microbiol. 39 (4), 219–225.
[53] Zopfi, J., Kjaer, T., Nielsen, L.P. and Jørgensen, B.B. (2001) Ecology of *Thioploca* spp.: Nitrate and sulfur storage in relation to chemical microgradients and influence of *Thioploca* spp. on the sedimentary nitrogen cycle. Appl. Environ. Microbiol. 67 (12), 5530–5537.
[54] Mußmann, M., Schulz, H.N., Strotmann, B., Kjaer, T., Nielsen, L.P., Rossello-Mora, R.A., Amann, R.I. and Jørgensen, B.B. (2003) Phylogeny and distribution of nitrate-storing *Beggiatoa* spp. in coastal marine sediments. Environ. Microbiol. 5 (6), 523–533.